

# GRAFTING POLYETHYLENE GLYCOL ON NANOCELLULOSE TOWARD BIODEGRADABLE POLYMER NANOCOMPOSITES

S. Geng,<sup>1</sup> K. Yao,<sup>2</sup> M. Harila,<sup>1</sup> Q. Zhou<sup>2</sup> and K. Oksman<sup>1,3\*</sup>

<sup>1</sup> Division of Materials Science, Department of Engineering Sciences and Mathematics, Luleå University of Technology, SE-971 87, Luleå, Sweden

<sup>2</sup> Royal Institute of Technology, School of Biotechnology, SE-100 44 Stockholm, Sweden

<sup>3</sup> Fibre and Particle Engineering, University of Oulu, FI-90014, Oulu, Finland

Email: [kristiina.oksman@ltu.se](mailto:kristiina.oksman@ltu.se)

Website: <https://www.ltu.se>

**Keywords:** Nanocellulose, Grafting, Dispersion, Mechanical property, Thermal property

## ABSTRACT

The reinforcing effect of a small amount of nanocellulose materials on biodegradable and polymer-based nanocomposites remains challenging because of the poor dispersion of the nanomaterials and inefficient interaction between the nanocellulose and the polymer matrix. To improve this, we grafted polyethylene glycol (PEG) on nanocellulose and produced composites of 0.1 wt% nanocellulose materials and polylactic acid (PLA) matrix. Here, two types of PEG grafted nanocellulose including TEMPO-oxidized cellulose nanocrystals (TOCNCs) and cellulose nanofibers (TOCNFs), with different lengths and diameters were used as reinforcements, respectively. We investigated the effects of grafting PEG on microstructure, mechanical properties and thermal behaviors of the PLA/nanocellulose composites. It is found that the PEG grafted nanocellulose dispersed better compared to the unmodified nanocellulose in the PLA matrix, and provides higher reinforcing effect that improves the elastic modulus of the nanocomposites compared to the composites with unmodified nanocellulose and ungrafted PEG. However, the glass transition temperature of the nanocomposites was not improved by grafting PEG significantly. We also found that the nanocomposites reinforced by TOCNF exhibited enhanced mechanical and thermal properties compared to those with TOCNCs, which is caused by the higher aspect ratio of the TOCNFs.

## 1 INTRODUCTION

Nanocellulose crystals or fibers are expected to be a promising reinforcement in polymer based nanocomposites due to their abundant resources, high integrity and biodegradable ability.[1] However, their reinforcing efficiency in some polymer matrices is limited, such as polylactic acid (PLA), because of the poor dispersion of them and the inefficient interaction between them and the matrix.[2] To improve this, many studies have been done on polymer grafting onto/from nanocellulose materials.[3-7] Harrison et al. has successfully grafted polystyrene (PS) and poly(tert-butyl acrylate) (Poly(TBA)) onto cellulose nanocrystals (CNCs), respectively, and the stability of the CNCs in organic solvents was improved.[3] Li et al. has grafted a copolymer of polylactic acid and glycidyl methacrylate (PLA-co-PGMA) onto bacterial cellulose (BC), and they suggested that this modified BC has improved compatibility with PLA compared to the unmodified BC.[4] Habibi et al. has investigated grafting polycaprolactone (PCL) on/from CNCs, resulting in enhanced elastic modulus and elongation to break of the PCL/CNC composites compared to those reinforced with unmodified CNCs.[5, 6] Braun et al. has reported that by grafting PLA from CNC surface hydroxyl groups, the resulted nanocomposites exhibit greatly improved heat distortion temperatures (up to 150 °C) relative to the pure PLA.[7]

In this study, covalent grafting polyethylene glycol (PEG) on nanocellulose was performed to improve the dispersion of nanocellulose as well as the interaction between nanocellulose and matrices in nanocomposites. Two types of nanocellulose materials were modified and used as reinforcements,

including 2,2,6,6-Tetramethylpiperidine-1-oxyl radical (TEMPO)-mediated oxidized cellulose nanocrystals (TOCNCs) and nanofibers (TOCNFs). Specifically, we concentrate on nanocomposites with a very low content of reinforcement (0.1 wt%), and we investigate the effects of grafting PEG on the microstructure, mechanical properties and thermal behaviors of the PLA/nanocellulose composites.

## 2 EXPERIMENTAL SECTION

### 2.1 Materials

2,2,6,6-tetramethyl-1-piperidinyloxy radical (TEMPO), sodium hydroxide, sodium bromide, sodium hypochlorite, methoxypolyethylene glycol amine (PEG,  $M_n = 750$ ), N-hydroxysuccinimide (NHS), 1-ethyl-3-(3-dimethylaminopropyl)carbodiimide hydrochloride (EDC) and N,N-dimethylformamide (DMF) were purchased from Sigma-Aldrich. Polylactic acid (Ingeo 4032D) was purchased from NatureWorks, Nebraska, USA. All chemicals and materials were used as received.

The TEMPO-oxidized cellulose nanocrystals (TOCNCs) were produced from a bioethanol processing followed with the TEMPO-mediated oxidation. The procedures were detailed described in our previous works.[8, 9] Briefly, the Norwegian spruce wood chips as starting materials were experienced an acid pre-treatment in a bioethanol pilot plant, and then were disintegrated through a high-pressure homogenizer and generated an aqueous cellulose nanocrystals suspension with *ca.* 2 wt% concentrations. Afterwards, TEMPO (16 mg/g cellulose), NaBr (100 mg/g cellulose) and NaClO (7.5 mmol/g cellulose) were added to the suspension and the pH of the suspension was controlled at 10 by 0.1M NaOH solution. Lastly, the suspension was washed using deionized water by filtration and a *ca.* 1 wt% TOCNC suspension was obtained.

The preparation of the TEMPO-oxidized cellulose nanofibers (TOCNFs) was described in our earlier work in detail.[10] Briefly, a commercial never-dried softwood sulphite pulp (kindly provided by Nordic Paper) was treated with a same TEMPO-mediated oxidation procedure as mentioned above, and a TOCNF suspension with 1.5 wt% solid content was obtained.

The PEG grafting process for both TOCNC and TOCNF was also demonstrated in our previous work.[10] In short, the EDC and NHS were added to the cellulose suspension and stirred for 30 min. Then, the PEG was added and the suspension was kept stirring for 24 h at room temperature or 37 °C and the pH was maintained between 7.5 and 8. Lastly, the pH of the suspension was changed to 1 and the PEG grafted nanocellulose suspension (coded as TOCNC-g-PEG and TOCNF-g-PEG) was then dialyzed in deionized water for purification. The weight fraction of the grafted PEG in the TOCNC-g-PEG is 38 wt% and that in the TOCNF-g-PEG is 33 wt% according to our previous thermogravimetric analysis.[9] The chemical structures of nanocellulose before and after PEG grafting are illustrated in Figure 1.

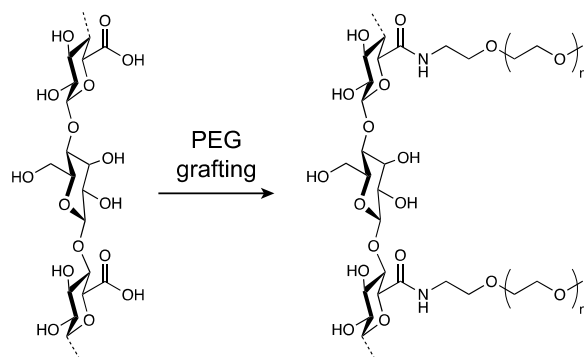


Figure 1: Chemical schematics of original TEMPO-oxidized nanocellulose and PEG grafted nanocellulose.

## 2.2 Preparation of nanocomposites

To prepare the nanocomposites with PEG grafted nanocellulose, the TOCNC-g-PEG or TOCNF-g-PEG suspension was added in DMF and stirred for 30 min, and then the PLA pellets were added in and stirred at 80 °C till totally dissolved. Afterwards, the obtained solution was poured into a Teflon petri dish and dried in an oven with a fan at 80 °C for 24 h. The dried film was then compressed using a laboratory press (LabEcon 300, Fontijne Grotnes, Netherlands) under a pressure 2.2 MPa at 190 °C for 1 min with 2 min pre-heating. To prepare the reference samples, the ungrafted TOCNC or TOCNF suspension and a certain amount of PEG that same as that of the grafted PEG were added into DMF instead, and then followed with same procedures mentioned above. The sample codes and compositions of all prepared nanocomposites in this study are shown in Table 1.

Sample coding	PLA (wt%)	Nanocellulose		PEG	
		Type	Content (wt%)	Type	Content (wt%)
PLA	100	-	0	-	0
0.1TOCNC/PEG	99.84	TOCNC	0.1	Ungrafted	0.06
0.1TOCNC-g-PEG	99.84	TOCNC	0.1	Grafted	0.06
0.1TOCNF/PEG	99.85	TOCNF	0.1	Ungrafted	0.05
0.1TOCNF-g-PEG	99.85	TOCNF	0.1	Grafted	0.05

Table 1: Compositions of the nanocomposites prepared in this study.

## 2.3 Characterizations

Fourier transform infrared (FTIR) spectroscopy was carried out using a Perkin-Elmer Spectrum 2000 FTIR equipped with MKII Golden Gate and single reflection attenuated total reflectance (ATR) system (Specac Ltd., London, UK). The samples were obtained from freeze drying of the aqueous suspensions and placed on an ATR crystal MKII heated diamond 45° ATR top plate. The spectral range of the measurements was from 600 to 4000 cm<sup>-1</sup> with a resolution of 4 cm<sup>-1</sup>.

Atomic force microscopy (AFM) was used to characterize the topography of the nanocellulose materials. The nanocellulose suspension was diluted to a certain concentration (10<sup>-4</sup> wt% for TOCNC and 10<sup>-3</sup> wt% for TOCNF), and then one droplet of the suspension was deposited on a fresh mica surface and dried overnight. Then the samples were scanned using the AFM tapping mode by a Veeco MultiMode scanning probe (Santa Barbara, USA) with Bruker TESPAs tips (Camarillo, USA).

Transmission electron microscopy (TEM) was performed on a Hitachi Model HT7700 transmission electron microscope using the high-resolution mode at 100 kV. To prepare the sample for TEM, a drop of the dilute nanocellulose suspension was deposited on a carbon-coated grid and then treated with 1% uranyl acetate negative stain.

Scanning electron microscopy (SEM) was performed using an FEI Magellan 400 XHR-SEM (Hillsboro, USA) to investigate the morphology of the fracture surfaces of the nanocomposite films after tensile testing. The fractured film was held vertically by two pieces of copper tape on an aluminum holder and coated with tungsten using a Bal-Tec MED 020 coating system. Then the secondary electron images were captured.

A universal testing machine (Shimadzu AG-X, Japan) was used to measure the mechanical properties of the nanocomposites with a SLBL-1kN load cell. At least 5 specimens of each sample were measured and the averages were calculated. All specimens were kept in a desiccator with 50 ± 5% humidity for 48 h, and then tested with a gauge length of 30 mm and a crosshead speed of 5 mm/min.

Dynamic mechanical analysis (DMA) was performed to measure the thermal properties of the samples using a Q800 analyzer (TA Instruments, New Jersey, USA) with a tension clamp configuration. The temperature ramps were executed in a range from room temperature to 100 °C with a scanning rate of 3 °C/min.

### 3 RESULTS AND DISCUSSION

#### 3.1 Structure and morphology of the unmodified and PEG grafted nanocellulose

The grafting of PEG on nanocellulose was confirmed by FTIR spectroscopy as shown in Figure 2. It can be seen from Figure 2a that after grafting PEG on TOCNC, the intensity of the band at  $1729\text{ cm}^{-1}$ , which is corresponding to the C=O stretching in acidic carboxyl groups,[11] was decreased because the grafting PEG consumed the amount of the carboxyl groups. Meanwhile, the intensity of the band at  $2894\text{ cm}^{-1}$  related to C–H stretching was higher in the TOCNC-g-PEG than in the TOCNC,[12] which is attributed to an increased number of methylene groups from the grafted PEG. Similarly, the TOCNF-g-PEG exhibits a band at  $1600\text{ cm}^{-1}$  corresponding to the C=O stretching in carboxylate ions with lower intensity compared to the unmodified TOCNF, while a band with higher intensity at  $2894\text{ cm}^{-1}$ .

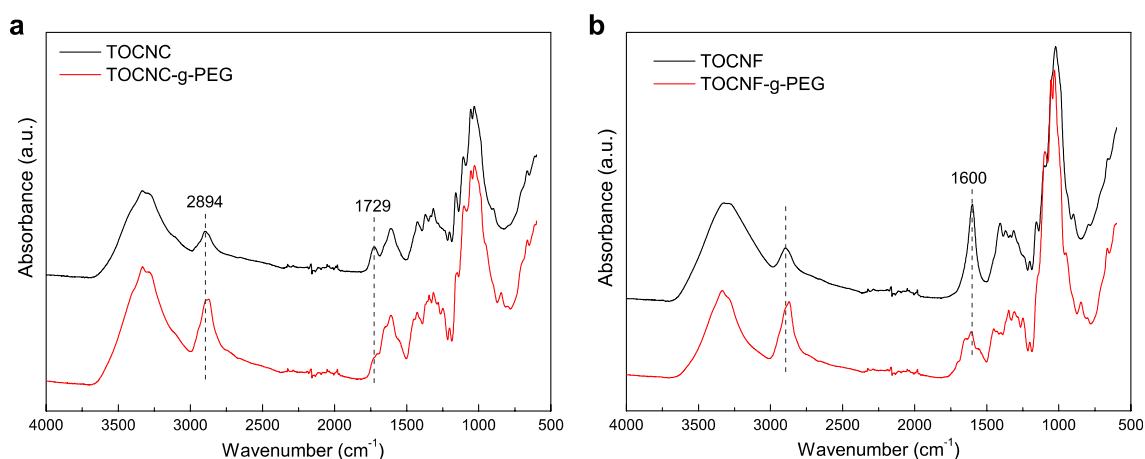


Figure 2: FTIR spectra of (a) TOCNC and TOCNC-g-PEG, and (b) TOCNF and TOCNF-g-PEG.

The morphology of the unmodified and PEG grafted nanocellulose materials was investigated by AFM as illustrated in Figure 3. The diameter and length of them were measured according to the TEM images using the “FiberApp” software,[13] and the results are shown in Table 2. Obviously, the TOCNF has smaller diameter and higher length, i.e., higher aspect ratio, compared to the TOCNC, and it tends to form more entanglements as shown in Figure 3 c and d. After grafting PEG, the diameters of the nanocellulose materials were increased slightly probably due to the PEG layer covered on the nanocellulose, and the length of them are very similar with the unmodified nanocellulose.

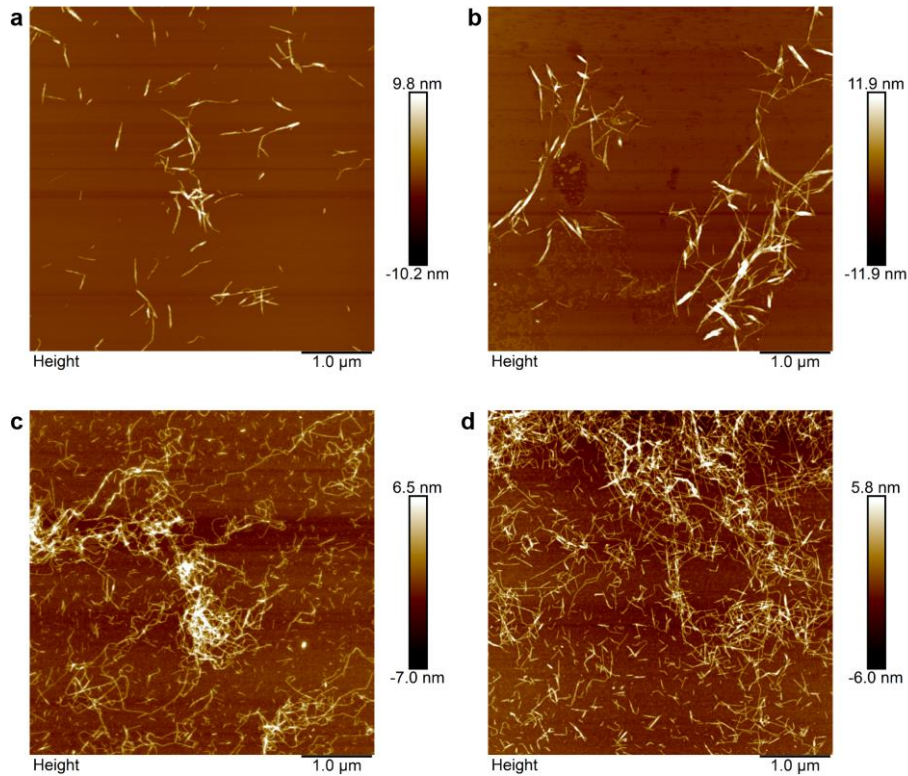


Figure 3: AFM height images of (a) TOCNC, (b) TOCNC-g-PEG, (c) TOCNF and (d) TOCNF-g-PEG.

Nanocellulose material	Diameter (nm)	Length (nm)
TOCNC	$5.7 \pm 1.2$	$570 \pm 280$
TOCNC-g-PEG	$6.3 \pm 1.4$	$520 \pm 280$
TOCNF	$3.6 \pm 0.7$	$820 \pm 570$
TOCNF-g-PEG	$4.3 \pm 0.6$	$830 \pm 480$

Table 2: Diameter and length of different nanocellulose materials measured by TEM.

### 3.2 Morphology of the PLA/nanocellulose composites

Turning to the morphology of the nanocomposite films, SEM was used to investigate the fracture surfaces of the samples after tensile testing. Figure 4 a and b show that there are some TOCNF aggregates in the 0.1TOCNF/PEG film, but less amount of aggregates presented in the 0.1TOCNF-g-PEG (Figure 4 c and d). This could imply that the dispersion of nanocellulose can be improved by grafting PEG, which is attributed to the steric effect coming from the PEG chains.[14]

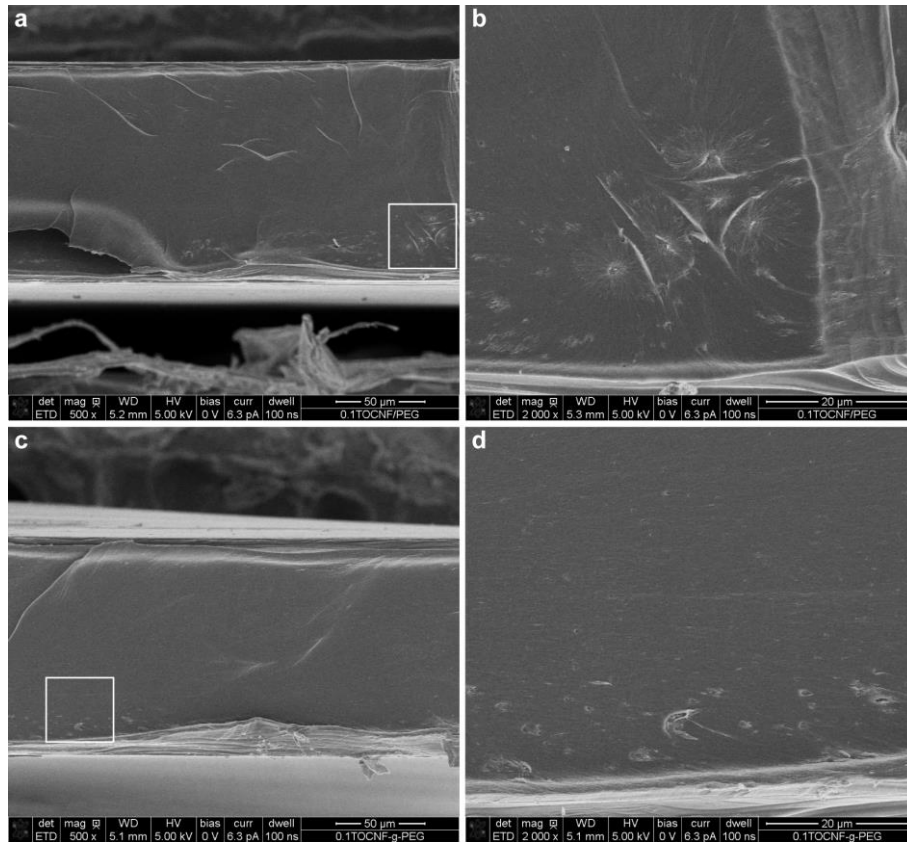


Figure 4: SEM images of the cross-sections of (a,b) 0.1TOCNF/PEG and (c,d) 0.1TOCNF-g-PEG films.

### 3.3 Mechanical properties of the composites

Mechanical properties of the nanocomposites were measured by tensile testing, and the obtained stress-strain curves are demonstrated in Figure 5 and the detailed data are shown in Table 3. We can see from Figure 5 that the elastic modulus of the PLA was increased slightly with adding 0.1 wt% TOCNFs, but the strength was decreased probably due to the plasticizing effect of PEG. The samples with 0.1 wt% TOCNFs show higher elastic modulus and strength compared to those with TOCNs, indicating TOCNF has higher reinforcing effect due to its higher aspect ratio. Moreover, the 0.1TOCNF-g-PEG exhibits higher elastic modulus, strength and elongation to break relative to the 0.1TOCNF/PEG, which is contributed to the better dispersion of the TOCNF-g-PEG in the PLA matrix as shown in Figure 4. In addition, the 0.1TOCNF-g-PEG composite indicates highest toughness among the prepared samples.

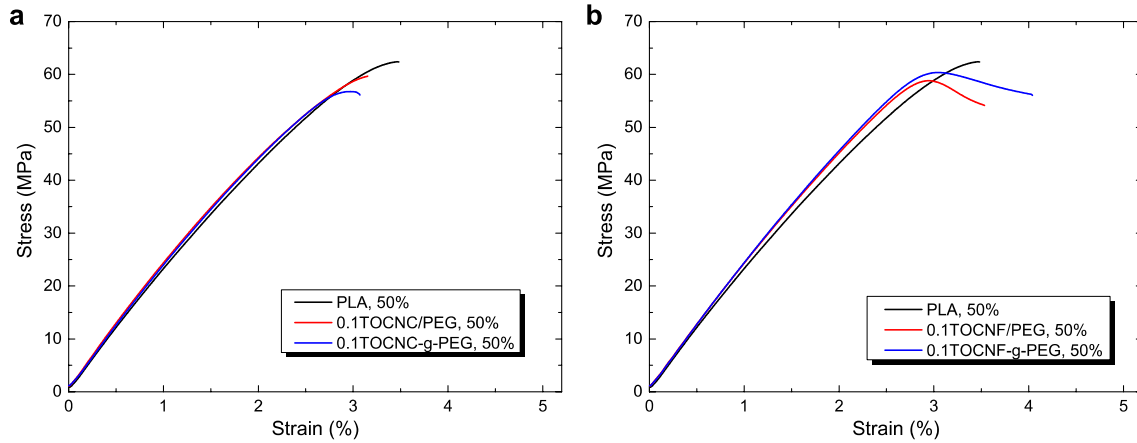


Figure 5: Stress-strain curves of pure PLA, (a) nanocomposites reinforced by TOCNCs and (b) nanocomposites reinforced by TOCNFs.

Sample coding	Humidity condition	Elastic modulus (GPa)	Yield strength (MPa)	Elongation at break (%)	Toughness (MJ/m <sup>3</sup> )
PLA	50%	2.15 ± 0.03	62.38 ± 0.92	3.48	1.26
0.1TOCNC/PEG	50%	2.19 ± 0.02	59.66 ± 0.83	3.15	1.09
0.1TOCNC-g-PEG	50%	2.20 ± 0.06	56.76 ± 2.63	3.07	1.03
0.1TOCNF/PEG	50%	2.24 ± 0.06	58.81 ± 1.82	3.53	1.31
0.1TOCNF-g-PEG	50%	2.27 ± 0.02	60.38 ± 1.35	4.04	1.63

Table 3: Mechanical properties of all composites measured by tensile testing.

### 3.4 Thermal behaviors of the composites

The thermal properties of the composites were analyzed by DMA and the results are shown in Figure 6. It can be seen that the storage modulus of the 0.1TOCNC-g-PEG is higher than the 0.1TOCNC/PEG because of the better dispersion of nanocellulose. The samples reinforced by TOCNFs have slightly higher storage modulus and glass transition temperature than those reinforced by TOCNCs due to the higher aspect ratio of TOCNFs. However, there is no obvious shift in glass transition temperature between ungrafted and PEG grafted nanocomposites.

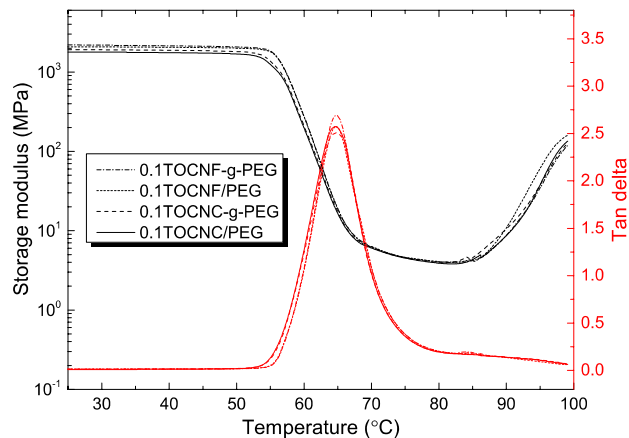


Figure 6: DMA analysis of 0.1TOCNC/PEG, 0.1TOCNC-g-PEG, 0.1TOCNF/PEG and 0.1TOCNF-g-PEG.

## 4 CONCLUSIONS

In conclusion, we have prepared PLA based nanocomposites with 0.1 wt% TOCNCs and TOCNFs, respectively. We studied the effects of grafting PEG on nanocellulose on the microstructure, mechanical properties and thermal behaviors of the nanocomposites. The grafting PEG was confirmed by FTIR spectroscopy, and the morphology of these two types of nanocellulose materials was characterized by AFM and TEM. We found that the grafting PEG can improve the dispersion of nanocellulose in PLA matrix, and further enhance the mechanical properties of the nanocomposites. Also, the TOCNF with higher aspect ratio provides higher reinforcing effect compared to TOCNC. The storage modulus of the samples follows similar tendency as the mechanical properties. However, there is no improvement of glass transition temperature achieved by grafting PEG. Further investigations on this subject will be performed.

## ACKNOWLEDGEMENTS

The authors thank for the financial support from Wallenberg Wood Science Center, SNS WOOD-PRO and Kempe Foundation.

## REFERENCES

- [1] S. Iwamoto, W. Kai, A. Isogai, T. Iwata, Elastic modulus of single cellulose microfibrils from tunicate measured by atomic force microscopy, *Biomacromolecules* **10**, 2009, pp. 2571-2576.
- [2] L. Suryanegara, A.N. Nakagaito, H. Yano, The effect of crystallization of PLA on the thermal and mechanical properties of microfibrillated cellulose-reinforced PLA composites, *Compos. Sci. Technol.* **69**, 2009, pp. 1187-1192.
- [3] S. Harrisson, G.L. Drisko, E. Malmström, A. Hult, K.L. Wooley, Hybrid rigid/soft and biologic/synthetic materials: polymers grafted onto cellulose microcrystals, *Biomacromolecules* **12**, 2011, pp. 1214-1223.
- [4] Z.Q. Li, X.D. Zhou, C.H. Pei, Synthesis of PLA-co-PGMA copolymer and its application in the surface modification of bacterial cellulose, *Int. J. Polymer. Mater.* **59**, 2010, pp. 725-737.
- [5] Y. Habibi, A. Dufresne, Highly filled bionanocomposites from functionalized polysaccharide nanocrystals, *Biomacromolecules* **9**, 2008, pp. 1974-1980.
- [6] Y. Habibi, A.-L. Goffin, N. Schiltz, E. Duquesne, P. Dubois, A. Dufresne, Bionanocomposites based on poly ( $\epsilon$ -caprolactone)-grafted cellulose nanocrystals by ring-opening polymerization, *J. Mater. Chem.* **18**, 2008, pp. 5002-5010.
- [7] B. Braun, J.R. Dorgan, L.O. Hollingsworth, Supra-molecular ecobionanocomposites based on polylactide and cellulosic nanowhiskers: synthesis and properties, *Biomacromolecules* **13**, 2012, pp. 2013-2019.
- [8] A.P. Mathew, K. Oksman, Z. Karim, P. Liu, S.A. Khan, N. Naseri, Process scale up and characterization of wood cellulose nanocrystals hydrolysed using bioethanol pilot plant, *Industrial Crops and Products* **58**, 2014, pp. 212-219.
- [9] T. Moberg, K. Sahlin, K. Yao, S. Geng, G. Westman, Q. Zhou, K. Oksman, M. Rigdahl, Rheological properties of nanocellulose suspensions: effects of fibril/particle dimensions and surface characteristics, *Cellulose* **24**, 2017, pp. 2499-2510.
- [10] H. Tang, N. Butchosa, Q. Zhou, A transparent, hazy, and strong macroscopic ribbon of oriented cellulose nanofibrils bearing poly (ethylene glycol), *Adv. Mater.* **27**, 2015, pp. 2070-2076.
- [11] M. Hasan, M. Zaki, L. Pasupulety, Oxide-catalyzed conversion of acetic acid into acetone: an FTIR spectroscopic investigation, *Applied Catalysis A: General* **243**, 2003, pp. 81-92.



- [12] S. Saini, D. Quinot, N. Lavoine, M.N. Belgacem, J. Bras,  $\beta$ -Cyclodextrin-grafted TEMPO-oxidized cellulose nanofibers for sustained release of essential oil, *J. Mater. Sci.* pp. 1-13.
- [13] I. Usov, R. Mezzenga, FiberApp: an open-source software for tracking and analyzing polymers, filaments, biomacromolecules, and fibrous objects, *Macromolecules* **48**, 2015, pp. 1269-1280.
- [14] J. Araki, M. Wada, S. Kuga, Steric stabilization of a cellulose microcrystal suspension by poly (ethylene glycol) grafting, *Langmuir* **17**, 2001, pp. 21-27.